Single-chain Variable Fragment Albumin Fusions Bind the Neonatal Fc Receptor (FcRn) in a Species-dependent Manner

IMPLICATIONS FOR IN VIVO HALF-LIFE EVALUATION OF ALBUMIN FUSION THERAPEUTICS*[S]

Jan Terje Andersen[‡§1], **Jason Cameron**[¶], **Andrew Plumridge**[¶], **Leslie Evans**[¶], **Darrell Sleep**[¶], **and Inger Sandlie**[‡§2]

From the [‡]Centre for Immune Regulation (CIR) and Department of Biosciences, University of Oslo, N-0316 Oslo, Norway, the [§]CIR and Department of Immunology, Oslo University Hospital Rikshospitalet and University of Oslo, Norway, PO Box 4950, N-0424 Oslo, Norway, and [¶]Novozymes Biopharma UK Limited, Castle Court, 59 Castle Boulevard, NG7 1FD Nottingham, United Kingdom

Background: Albumin is utilized as carrier of biopharmaceuticals. FcRn binding regulates its long half-life.
Results: ScFv fusion to HSA only slightly reduces human FcRn binding, whereas HSA and scFv-HSA fusions have very weak binding to rodent FcRn.
Conclusion: Rodents have limitations for preclinical evaluation of HSA fusions.
Significance: We illuminate design of HSA fusions and highlight cross-species differences to consider prior to preclinical evaluation.

Albumin has a serum half-life of 3 weeks in humans. This has been utilized to extend the serum persistence of biopharmaceuticals that are fused to albumin. In light of the fact that the neonatal Fc receptor (FcRn) is a key regulator of albumin homeostasis, it is crucial to address how fusion of therapeutics to albumin impacts binding to FcRn. Here, we report on a detailed molecular investigation on how genetic fusion of a short peptide or an single-chain variable fragment (scFv) fragment to human serum albumin (HSA) influences pH-dependent binding to FcRn from mouse, rat, monkey, and human. We have found that fusion to the N- or C-terminal end of HSA only slightly reduces receptor binding, where the most noticeable effect is seen after fusion to the C-terminal end. Furthermore, in contrast to the observed strong binding to human and monkey FcRn, HSA and all HSA fusions bound very poorly to mouse and rat versions of the receptor. Thus, we demonstrate that conventional rodents are limited as preclinical models for analysis of serum half-life of HSA-based biopharmaceuticals. This finding is explained by cross-species differences mainly found within domain III (DIII) of albumin. Our data demonstrate that although fusion, particularly to the C-terminal end, may slightly reduce the affinity for FcRn, HSA is versatile as a carrier of biopharmaceuticals.

A plethora of therapeutically promising proteins, such as hormones, growth factors, cytokines, coagulation factors, enzymes, peptides, antibody-derived fragments, and novel protein scaffolds, is either approved for therapy or currently in clinical development (1–3). Despite encouraging results from *in vitro* cellular experiments, the therapeutic effect of many is often limited as a result of poor pharmacokinetics, mainly as a consequence of fast elimination from the body. The main reason is their molecular size, below the kidney clearance threshold (<60 kDa), and susceptibility to rapid degradation by serum and intracellular proteases.

Several strategies have been developed to extend serum persistence. One is the use of chemical conjugation of polyethylene glycol (PEGylation) to the drug or interest, which increases the hydrodynamic radius and decreases kidney clearance (4). Another approach is the use of small albumin binding domains, peptides, or fatty acids fused or conjugated directly to the drug that target serum albumin when injected into the bloodstream (5–11).

Albumin (molecular mass 66.7 kDa, above kidney threshold) has a serum half-life of 3 weeks in humans. The feature is shared with the IgG class of antibodies, and both albumin and IgG bind to a cellularly expressed receptor, named the neonatal Fc receptor (FcRn),[3] which regulates their half-life (12, 13). They bind to different binding sites, may bind FcRn simultaneously, and do so in a noncooperative manner. Binding to both ligands is strictly pH-dependent, with binding at acidic pH (pH 6.0) and no binding or release at physiological pH (14–16). Both binding interfaces contain conserved histidine residues, located to the IgG Fc, domain III (DIII) of albumin as well as the receptor, which becomes positively charged at acidic pH (15, 16). The pH dependence of the interaction is a prerequisite for efficient FcRn-mediated rescue of the ligands from intracellular degradation. Rescue occurs via a recycling pathway, where FcRn, predominantly located within acidified endosomes, binds its ligands taken up by pinocytosis (16). Ligand binding at acidic

[1] To whom correspondence may be addressed: CIR and Dept. of Immunology, Oslo University Hospital Rikshospitalet and University of Oslo, P. O. Box 4956, Oslo N-0424, Norway. E-mail: j.t.andersen@imbv.uio.no.
[2] To whom correspondence may be addressed: CIR and Dept. of Immunology, Oslo University Hospital Rikshospitalet and University of Oslo, PO Box 4956, Oslo N-0424, Norway. E-mail: inger.sandlie@imbv.uio.no.

[3] The abbreviations used are: FcRn, neonatal Fc receptor; hFcRn, human FcRn; mFcRn, mouse FcRn; rat FcRn, rFcRn; myFcRn, rhesus monkey FcRn; HSA, human serum albumin; MSA, macaque serum albumin; RSA, rat serum albumin; mySA, rhesus monkey serum albumin; DIII, domain III; DII, domain II; DI, domain I; scFv, single-chain variable fragment; Bis-Tris, 2-(bis(2-hydroxyethyl)amino)-2-(hydroxymethyl)propane-1,3-diol; RU, resonance units.

pH results in transport back to the cell surface, where exposure to the neutral pH of the blood triggers release of IgG and albumin back into the circulation. Proteins that do not bind FcRn are lysosomally degraded. The receptor-mediated recycling mainly takes place in hematopoietic cells and endothelial cells lining the vascular space. Thus, FcRn-mediated rescue offers an opportunity to extend or modulate serum half-life of therapeutic antibodies or biopharmaceuticals targeted or fused to albumin. The latter can be done by coupling of a protein of interest to albumin, chemically or genetically (3, 9, 17–19). Regardless of the strategy chosen, it is crucial for enhanced half-life that pH-dependent binding to FcRn is not disrupted.

Direct genetic fusion of biopharmaceuticals to full-length human serum albumin (HSA) has been explored for some time, and a wide range of different small therapeutic proteins has been genetically fused to either the N-terminal or the C-terminal end (3, 9, 10, 17, 18). Preclinical evaluations of their pharmacokinetics have been extensively performed in rodents, and improved serum half-lives as compared with nonfused counterparts have been demonstrated, as reviewed elsewhere (20). However, half-lives have been far from that of the endogenous albumin of the animals used. Notably, such studies were carried out before the role of FcRn and its impacts on half-life regulation of albumin were appreciated.

To obtain efficient FcRn-mediated recycling and optimal pharmacokinetics of the next generation of HSA fusions, knowledge of whether or not fusion interferes with binding to FcRn is absolutely required. Therefore, we aimed to investigate how genetic fusion to either the N-terminal or the C-terminal end of HSA affects pH-dependent binding to human FcRn (hFcRn). Furthermore, as preclinical evaluations of such fusions are frequently carried out in rodents prior to assessment in non-human primates, we studied how the HSA fusions bound to mouse, rat, and rhesus monkey FcRn. Our data reveal that fusions of a peptide- or an antibody-derived single-chain variable fragment (scFv) to the N- or C-terminal end of HSA have only minor negative impact on binding to the rhesus monkey and human forms of FcRn. Furthermore, fundamental differences in binding properties were detected across species, which could compromise the use of conventional rodents as models for *in vivo* evaluation of HSA-based biopharmaceuticals. Finally, the differences in binding observed between the species were explained by nonconserved amino acids, mainly found within DIII of albumin.

EXPERIMENTAL PROCEDURES

Production of Recombinant FcRn Molecules—The construction of eukaryotic vectors encoding recombinant truncated forms of human, mouse, and rat FcRn that contain cDNAs for the three extracellular domains ($\alpha 1-\alpha 3$) C-terminally fused to a gene encoding the *Schistosoma japonicum* glutathione *S*-transferase (GST) has been described previously (21, 22). A cDNA fragment encoding a truncated version of the rhesus monkey (*Macaca mulatta*; accession numbers AFI34748) FcRn heavy chain (GenScript), was subcloned and produced as described (22). All vectors contain a cDNA encoding human β_2-microglobulin and the Epstein-Barr virus origin of replication sequence. Soluble forms of FcRn were produced by transient transfection of human embryonic kidney 293E cells with the vectors described above using Lipofectamine 2000 (Invitrogen). Harvested supernatants were pooled, and secreted receptors were purified using a GSTrap FF column as described previously (23).

Construction of HSA Fusions—*Escherichia coli* DH5α was used for the general manipulation, propagation, and preparation of DNA (24). Plasmids containing expression cassettes for the production of scFv genetically fused to HSA, at either the N terminus or the C terminus or both, and a FLAG (FG) sequence (DYKDDDDK) genetically fused to HSA were used as described (25). Expression plasmids were used to transform *Saccharomyces cerevisiae* D638 cir^0 (*pmt1* mutant derived of DYB7) using methods described (25, 26). An expression cassette containing the FLAG tag genetically fused to the N terminus of HSA was prepared using PCR and *in vivo* cloning (*i.e.* gap repair in yeast). Two DNA fragments were amplified by PCR using Phusion polymerase (New England Biolabs), as per the manufacturer's instructions, from plasmid pDB3927 (15), and oligonucleotide pairs xAP032/xAP353 (fragment 1) and xAP033/xAP354 (fragment 2) (supplemental Tables 1 and 3). Fragment 1 (2.465 kb) contained the *S. cerevisiae LEU2* ORF and 3'-UTR, *S. cerevisiae PRB1* promoter, DNA encoding a leader sequence (MKWVS-FISLLFLFSSAYSRSLDKR), and FLAG tag. Fragment 2 (2.240 kb) contained DNA encoding the FLAG tag (sharing 27 bp homology with the 3' region of PCR fragment 1), HSA, the *S. cerevisiae ADH1* terminator, and 459 bp of flanking DNA from the plasmid backbone. Both PCR fragments were purified using a Qiagen PCR purification kit according to the manufacturer's instructions. A second round PCR step was carried out to fuse fragments 1 and 2 and to subsequently amplify the spliced product. The PCR mix contained 20 μl of HF buffer (New England Biolabs), 2 μl of dNTP (10 mM each), 1 μl of oligonucleotides (1 μM) xAP072/xAP262 (supplemental Table 3), 1 μl of each purified fragment, 1 μl of Phusion polymerase, and 71 μl of distilled H_2O. PCR cycling was carried out according to the manufacturer's instructions. The 3.358-kb spliced PCR product was digested with NgoMIV/AvrII, and the 1.977-kb product (containing the 3' region of the *S. cerevisiae PRB1* promoter, nucleotide sequence encoding FL, the FLAG tag, and the majority of HSA) was ligated into NgoMIV/AvrII-digested pDB3927 to create pDB4643. pDB4643 was digested with NsiI/PvuI, and the DNA was purified using a Qiagen PCR purification kit as per the manufacturer's instructions before being used, along with Acc65I/BamHI-digested pDB3936, to co-transform *S. cerevisiae* D638 cir^0 as described (15, 26).

Construction and production of N- and C-terminal fusions of an scFv fragment with specificity to fluorescein isothiocyanate (FITC) have previously been described (25). All fusions of scFv to the C terminus of HSA have a linker, $(GGS)_4GG$, referred to as *GS* in Fig 1.

Construction of Mouse, Rat, and Rhesus Monkey Albumin—Expression cassettes for mouse, rat, and rhesus macaque albumin (MSA, RSA, and MySA) (accession numbers: BC024643, BC085359, and NP_001182578.1, respectively) were prepared by GeneArt GmbH. Expression cassettes (NotI fragments) contained the *S. cerevisiae PRB1* promoter, nucleotide sequence encoding the leader sequence, and a codon-optimized gene encoding MSA, RSA, or MySA in frame of an *S. cerevisiae*

ADH1 terminator. NotI expression cassettes were ligated into NotI-digested pSAC35 to create pDB3442, pDB3444, and pDB4118, respectively, and *S. cerevisiae* D638 cir[0] was transformed as described (15).

The HSA C-terminal amino acids from positions 573 to 585 (KKLVAASQAALGL) were changed to those in MSA (PNLVTRCKDALA) by insertion of a synthetic DNA fragment (SacI/SphI) (DNA2.0 Inc.) by gene assembly and subcloning into SacI/SphI-digested pDB3927 (15) to produce plasmid pDB4115. The expression plasmid was generated *in vivo* (*i.e.* gap repair) as described (15).

Plasmids for chimeric variants of MSA and HSA (MSA DI + DII (amino acids 1–380) + HSA DIII (amino acids 381–585) and HSA DI + DII (amino acids 1–380) + MSA DIII (amino acids 381–584)) were generated using PCR and *in vivo* cloning. PCR was used to amplify two PCR fragments from template DNA (supplemental Tables 2 and 3). Fragment 1 contained the *LEU2* ORF and 3′-UTR, *PRB1* promoter, the DNA encoding the leader sequence, DI+DII of parent albumin (*e.g.* from human or mouse), and 27–30 bp of DNA encoding DIII of donor albumin. Fragment 2 contained the DNA-encoding DIII of donor albumin, the *ADH*t terminator, and 217-bp flanking sequence homologous with nucleotide sequence in pDB3936 (22). *S. cerevisiae* D638 cir[0] (26) was co-transformed with both PCR fragments and Acc65I/BamHI-digested pDB3936 by gap repair as described (15).

Yeast Production of Albumin—Albumin variants were purified from cultures using an albumin affinity matrix (AlbuPure®, ProMetic BioSciences, Inc.) as described previously (15). Albumins were chromatographed in 25 mM sodium phosphate, 100 mM sodium sulfate, 0.05% (w/v) sodium azide, pH 7.0, at 1 ml/min and quantified by UV detection at 280 nm, relative to an HSA standard. Using precast NuPAGE 4–12% Bis-Tris gels and MOPS SDS buffer (Invitrogen), samples of 1 μg were diluted 1:1 with reducing sample buffer (NuPAGE LDS sample buffer) and heated to 70 °C for 5 min. Electrophoresis was performed for 50 min at 200 V, and gels were stained with InstantBlue protein stain (Expedeon).

ELISA—MaxiSorp microtiter wells (Nunc) were coated with 100 μl of FITC-conjugated to a goat Fab$_2$ fragment (Abcam) or an anti-FLAG mouse IgG antibody (Sigma-Aldrich) at 1 μg/ml, incubated overnight at 4 °C, and then blocked with and blocking with 4% skimmed milk (Acumedia) for 1 h at room temperature. Then, the wells were washed four times with PBS, 0.005% Tween 20, pH 7.4 (PBS/T), 4% skimmed milk (Acumedia) for 1 h at room temperature and washed four times with PBS/T. Serial dilutions of HSA variants (5–0.04 μg/ml) were added to the wells for 1 h and then washed as above. Then, a horseradish peroxidase-conjugated anti-HSA antibody preparation (Abcam) diluted in 4% skimmed milk PBS/T was added and incubated for 1 h prior to washing as above. Subsequently, binding was visualized using the 3,3′,5,5′-tetramethylbenzidine substrate (Calbiochem).

SPR—SPR analyses were performed on a BIAcore 3000 instrument (GE Healthcare), and CM5 chips where immobilized with GST-tagged mouse FcRn (mFcRn), rat FcRn (rFcRn), rhesus monkey FcRn (myFcRn), or hFcRn using the amine coupling kit (GE Healthcare) where receptor samples (10 μg/ml) were injected in 10 mM sodium acetate at pH 5.0 (GE Health-

care), all as described by the manufacturer. Unreacted moieties on the CM5 surface were blocked with 1 M ethanolamine. For all experiments, phosphate buffer (67 mM phosphate buffer, 0.15 M NaCl, 0.005% Tween 20) at pH 6.0 or 7.4 or HBS-P buffer (0.01 M HEPES, 0.15 M NaCl, 0.005% surfactant P20) at pH 7.4 were used as running buffer or dilution buffer. Relative binding was measured by injecting 10 μM of each of the albumin variants at either pH 6.0 or pH 7.4. Kinetic measurements were performed using serial dilutions of albumin variants (20.0–0.3 or 200.0–3.1 μM) injected using buffer with pH 6.0 or 7.4, at a flow rate of 50 μl/min at 25 °C. Competitive binding was measured by injecting hFcRn (50 nM) alone or together with different amounts of HSA or HSA fusions (900.0–0.03 nM) over immobilized HSA (~2000 RU). In all experiments, to correct for nonspecific binding and bulk buffer effects, responses obtained from the control CM5 surfaces and blank injections were subtracted from each interaction curve. Kinetic rate values were calculated using the simple Langmuir 1:1 ligand binding model provided by the BIAevaluation 4.1 software. The closeness of the fit, described by the statistical value χ^2, which represents the mean square, was lower than 2.0 in all affinity estimations.

RESULTS

Albumin Fusion Formats—To address how genetic fusion of proteins to HSA affects binding of HSA to FcRn, several HSA fusion variants were constructed using a synthetic *HSA* gene that is codon-optimized for expression in *S. cerevisiae* (25). A model peptide HSA fusion was constructed by adding the sequence corresponding to the FLAG tag (DYKDDDDK (2 kDa)) to the N- or C-terminal end, whereas an scFv fragment (12 kDa) with specificity for FITC was fused to either the N-terminal or the C-terminal end or both. ScFv fused to the C terminus of albumin included a linker sequence ((GGS)$_4$GG) inserted between HSA and the scFv fragment and a FLAG tag at the C-terminal end of scFv. In addition, fusions were made that contained a K500A point mutation within DIII (HSA[K500A]-FG and scFv-HSA[K500A]-FG) as this point mutation was previously shown to reduce binding to hFcRn by more than 30-fold (15). A schematic overview of the different fusion formats is shown in Fig. 1, *A* and *B*.

All HSA fusions were expressed from the *S. cerevisiae PRB1* promoter, and a leader sequence was fused in-frame to the *HSA* gene. Monomeric nonfused and fused albumin variants were obtained following purification using an AlbuPure® albumin affinity matrix. SDS-PAGE analysis followed by Coomassie Brilliant Blue staining revealed distinct bands with molecular weights corresponding to their expected sizes (Fig. 1*C*).

Binding Integrity of HSA-fused Molecules—A prerequisite for the use of HSA as a carrier of small therapeutics is that the fused molecules retain their proper folding and functional binding to their target. To test the integrity of the fused molecules, ELISAs were carried out where the FLAG-tagged fusions were captured on a monoclonal anti-FLAG antibody coated in wells followed by detection using an enzyme-conjugated anti-HSA antibody. Both N-terminal and C-terminal FLAG fusions as well as the K500A mutants bound equally well to the anti-FLAG antibody (Fig. 2*A*). Similarly, sandwich ELISA, with capture of the scFv
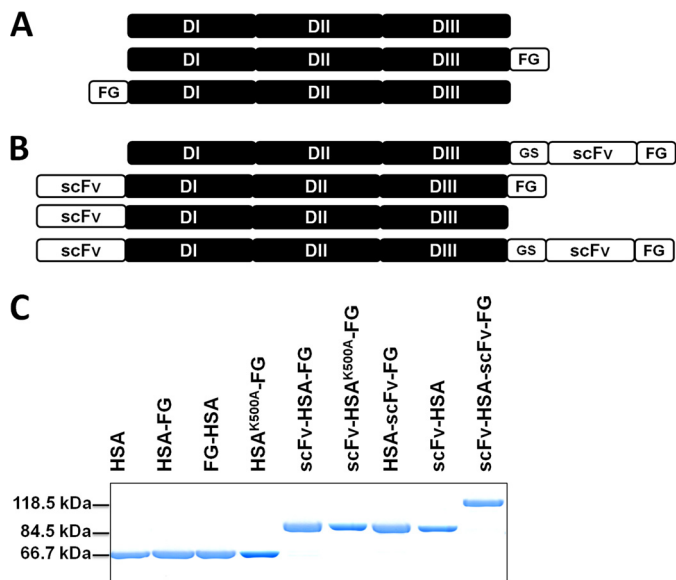
FIGURE 1. **HSA fusion formats.** *A* schematic illustrations of nonfused HSA with its three subdomains DI, DII, and DIII, HSA with a C-terminal FLAG tag (HSA-FG), and HSA with an N-terminal FLAG tag (FG-HSA). *B*, schematic illustrations of HSA with a C-terminal scFv followed by a FLAG tag (HSA-scFv-FG), HSA with an N-terminally fused scFv and a C-terminal FLAG tag (scFv-HSA-FG), HSA with an N-terminally fused scFv (scFv-HSA), and a bivalent HSA with an scFv fragment fused to both the N-terminal and the C-terminal end (scFv-HSA-scFv-FG). All scFv fusions have a glycine-serine linker ((GGS)$_4$GG, referred to as *GS*) inserted between the C terminus of HSA and the scFv. *C*, HSA and HSA fusions produced in *S. cerevisiae* and subsequently purified on an albumin affinity matrix were analyzed by 12%(w/v) SDS-PAGE.

fusions on FITC-conjugated Fab$_2$ fragments coated in wells, showed that fusions of scFv added to either end of HSA or both retained binding (Fig. 2*B*). Thus, we conclude that the HSA fusion partners are functionally folded.

Binding of HSA Fusions to hFcRn—We compared the two sets of fusions with nonfused HSA for binding to FcRn. All were injected in equimolar amounts over hFcRn immobilized on a CM5 chip at pH 6.0, and fusions involving WT HSA were shown to bind the receptor in a reversible manner, like that of nonfused HSA (Fig. 3, *A–D*), whereas only weak binding was detected for HSA^{K500A}, HSA^{K500A}-FG, and scFv-HSA^{K500A}-FG. When comparing the relative binding responses of the fusion variants with that of WT HSA, C-terminal fusions were shown to bind slightly less than the N-terminal fusions, although no major reduction in binding capacity was observed for any of the fusions.

To quantify the differences in binding of the fusions, we performed kinetic analysis, where serial dilutions of the HSA variants were injected over immobilized hFcRn at acidic pH. The kinetic values were calculated by fitting the sensorgrams to a simple first-order 1:1 Langmuir bimolecular interaction model. The derived kinetics revealed minor, but distinct, differences between the fusion variants and nonfused HSA, which reflect the relative binding responses. The most noticeable effect was again detected for the C-terminal fusions that at most showed a near 2-fold reduction in K_D (Table 1). Notably, C-terminal fusion of a short FLAG peptide had the same impact as fusion of the larger scFv domain. N-terminal fusion of either FLAG tag or scFv had very little effect.

Competitive FcRn Binding—HSA is the most abundant protein in blood, and biopharmaceuticals fused to HSA must necessarily compete with large amounts of endogenous HSA for binding to hFcRn. To investigate the ability of the fusions to compete for binding to the receptor, we compared how FLAG and scFv fusions bound hFcRn in the presence of WT HSA, using an established SPR-based assay. Here, WT HSA was immobilized on a CM5 biosensor chip, and a constant amount of hFcRn was injected at pH 6.0 in the presence of titrated amounts of HSA or HSA fusions. As compared with WT HSA, both fusions showed a slightly reduced capacity to compete for binding to the receptor (Fig. 4, *A* and *B*), which reflects the small differences in kinetics. Furthermore, the single K500A point mutation, introduced into both fusion formats, almost completely eliminated their ability to compete for binding. Thus, fusion of a short peptide or an antibody-derived scFv to the C-terminal end of HSA was shown to only slightly reduce the capacity to compete for binding to hFcRn.

Binding of Albumin Species and HSA Fusions to Mouse, Rat, and Rhesus Monkey FcRn—Preclinical pharmacokinetic evaluations of HSA fusions are routinely performed in rodents followed by studies in non-human primates. However, no studies so far have addressed the impact of the fusions on HSA binding to FcRn from the animals used. Therefore, we compared the binding activities of the HSA fusions to soluble forms of recombinant mFcRn, rFcRn, and myFcRn. In addition, we constructed and produced monomeric fractions of MSA, RSA, and MySA using the yeast expression system. The purified albumin fractions showed the expected molecular weights on an SDS-PAGE gel (supplemental Fig. S1).

Again, SPR with immobilized receptors was carried out using equal molar amounts of HSA, MySA, RSA, or MSA injected at pH 6.0. All variants bound hFcRn reversibly, but distinct differences in binding profiles were observed (Fig. 3, *A* and *E–G*). The strongest binding was to MSA followed by RSA, due to slower dissociation. MySA had a slightly reduced binding capacity as compared with HSA.

Furthermore, myFcRn bound more strongly to MySA than to HSA, whereas MSA and RSA bound better than MySA (Fig. 5, *A* and *E–G*). The mouse and rat forms of FcRn bound weakly to MySA and HSA as compared with strong binding to MSA and RSA (Fig. 6, *A* and *E–G*, and supplemental Fig. S2). The near lack of binding seen for nonfused HSA toward mFcRn was also seen for all HSA fusion molecules. A similar trend was seen for binding to rFcRn (supplemental Fig. S2). Thus, the rodent receptors bind only very weakly to HSA and HSA fusions.

Swapping of Albumin Domains Reveal Cross-species Binding Differences—We have previously shown that the C-terminal DIII of HSA is crucial for binding to hFcRn (15). Thus, to investigate why HSA binds poorly to mFcRn, we constructed chimeric variants of HSA and MSA, where the C-terminal DIII of HSA was fused to DI-DII of MSA and *vice versa* (HSA-DIIIm and MSA-DIIIh) and expressed the variants in yeast (Fig. 7*A*). Then, binding to FcRn was evaluated by SPR, where the variants were injected over the human and mouse forms of FcRn. We found that the affinity of HSA-DIIIm to hFcRn improved considerably as compared with HSA (Fig. 7*B*). Interestingly, it also bound more strongly than WT MSA, with a K_D of 0.1 μM, 8-fold stronger than that previously reported for the hFcRn-MSA interaction (22). Swapping of DIII from HSA onto DI-DII from
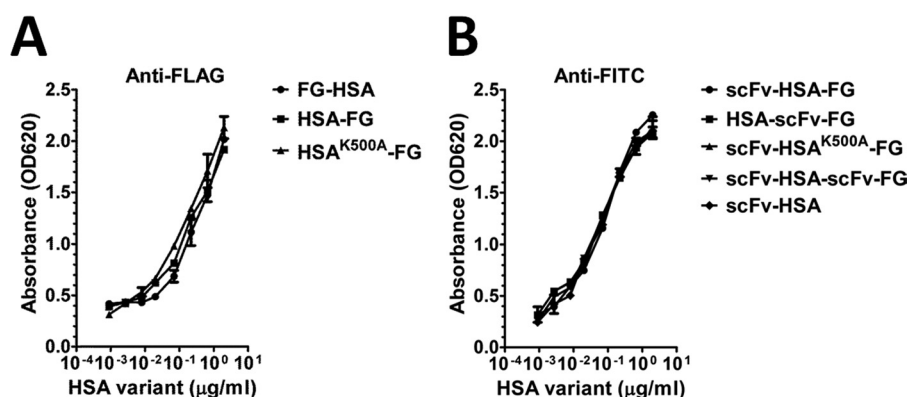
FIGURE 2. **Binding integrity of HSA fusions.** *A*, binding of serial dilutions of FLAG-tagged HSA fusion variants to an anti-FLAG antibody coated in wells. *B*, binding of serial dilutions of anti-FITC scFv-fused HSA variants to an FITC-conjugated Fab$_2$ fragment coated in wells. Binding of HSA variants were visualized using an HRP-conjugated anti-HSA antibody. The numbers given represent the mean of triplicates. *Error bars* indicate S.D. *OD*, optical density.
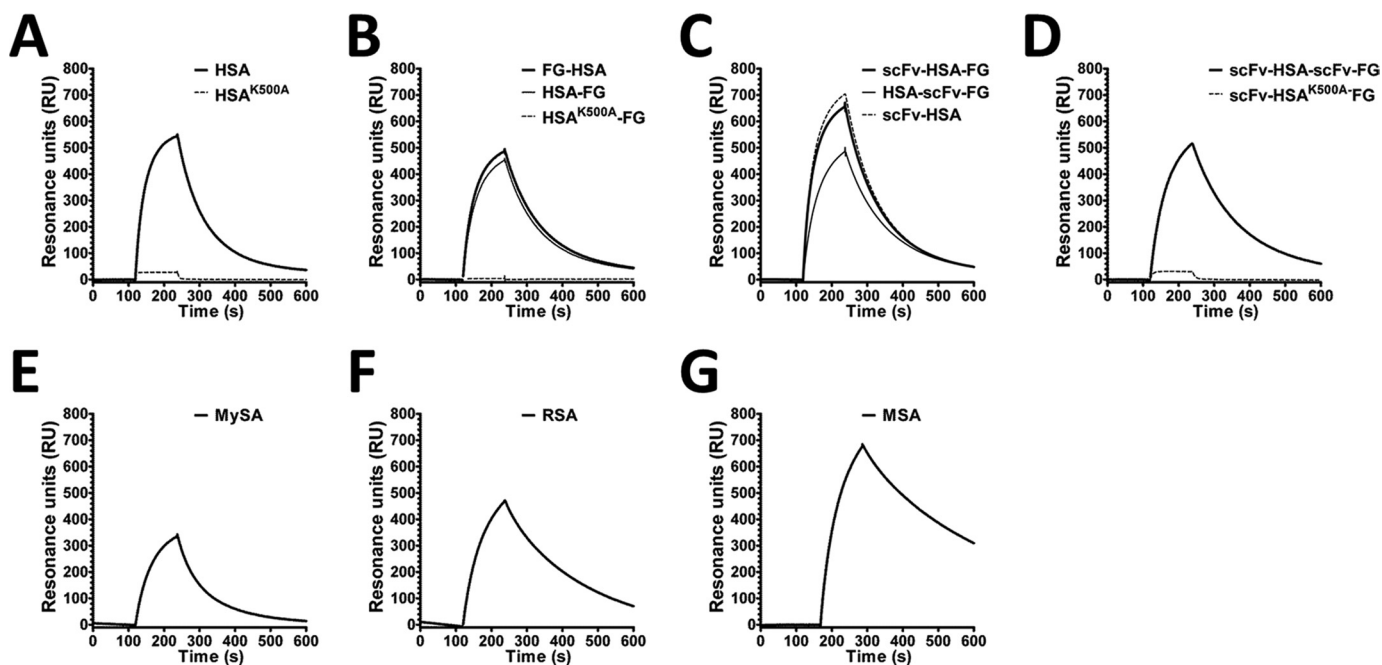

FIGURE 3. **Functional binding of albumin variants to human FcRn.** *A–G*, representative sensorgrams showing binding of 1 μM HSA and HSA^{K500A} (*A*), FG-HSA, HSA-FG, and HSA^{K500A}-FG (*B*), scFv-HSA-FG, HSA-scFv-FG, and scFv-HSA (*C*), scFv-HSA-scFv-FG and scFv-HSA^{K500A}-FG (*D*), MySA (*E*), RSA (*F*), and MSA (*G*) injected over hFcRn immobilized on a CM5 chip (~1000 RU) at pH 6.0. Injections were performed at 25 °C, and the flow rate was 50 μl/min.

TABLE 1

Binding kinetics of HSA-fusion interactions with human FcRn

The kinetic values represent the average of triplicates.

HSA variant[a]	k_a	k_d	K_D[b]
	$10^3/ms$	$10^{-3}/s$	μM
HSA	5.5 ± 0.1	6.5 ± 0.2	1.1
HSA-FG	3.9 ± 0.2	7.4 ± 0.1	1.9
FG-HSA	7.1 ± 0.0	8.1 ± 0.1	1.1
scFv-HSA	5.2 ± 0.2	6.7 ± 0.1	1.2
scFv-HSA-FG	4.5 ± 0.1	7.4 ± 0.0	1.6
HSA-scFv-FG	4.3 ± 0.1	7.4 ± 0.1	1.7
scFv-HSA-scFv-FG	4.2 ± 0.1	7.7 ± 0.1	1.8

[a] Dilutions of HSA variants were injected over immobilized hFcRn (~1000 RU).
[a] The kinetic rate constants were obtained using a simple first-order (1:1) bimolecular interaction model.

MSA (MSA-DIIIh) resulted in the opposite effect, with a significant reduction in binding to hFcRn (Fig. 7*B*). Moreover, when binding of the chimeric MSA-DIIIh and HSA-DIIIm variants was tested toward mFcRn, HSA-DIIIm was shown to bind almost equally well as MSA, whereas MSA-DIIIh bound poorly

(Fig. 7*C*). Thus, sequence variations found within DIII are major contributions to the large cross-species binding differences, whereas variations found outside DIII may have a minor effect.

Furthermore, we addressed the impact of the last 25 amino acids of the C-terminal acid α-helix of DIII as we have previously shown that truncation of this stretch of amino acids resulted in loss of binding to hFcRn (15). To do so, we exchanged this part of MSA onto HSA (HSA-Cm), tested the binding capacity toward mFcRn, and found that binding was improved as compared with WT HSA (Fig. 7*D*). In conclusion, DIII of albumin is for the most part responsible for the cross-species FcRn binding differences observed, and the C-terminal end of albumin plays a critical role.

DISCUSSION

HSA has emerged as a versatile carrier for therapeutic and diagnostic agents, and recombinant technology allows for genetic fusion of HSA to either the N-terminal or the C-termi-
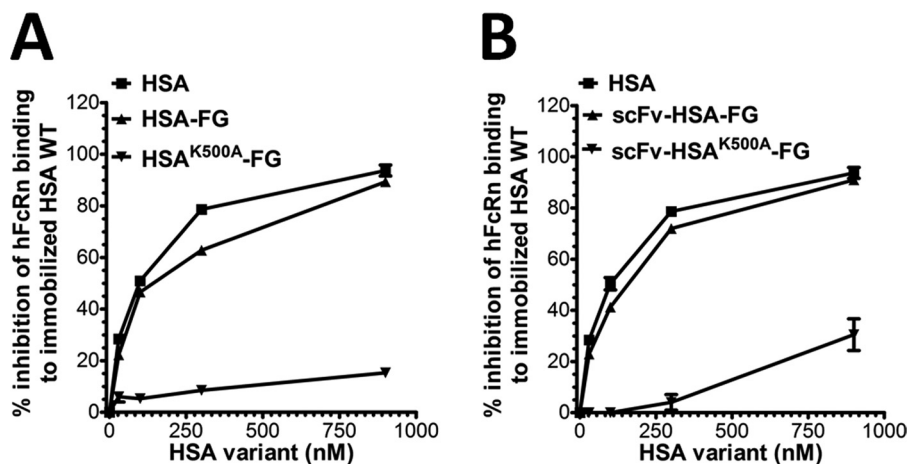
FIGURE 4. **Competitive HSA-human FcRn binding.** *A*, serial dilutions of equal amounts (900 – 0.03 nM) of HSA, HSA-FG, and HSA^{K500A}-FG were preincubated with hFcRn (0.05 μM) and injected over immobilized HSA at pH 6.0. *B*, serial dilutions of equal amounts (900 – 0.03 nM) of HSA, scFv-HSA-FG, scFv-HSA-FG, and scFv-HSA^{K500A}-FG were preincubated with hFcRn (0.05 μM) and injected over immobilized HSA at pH 6.0. Injections were performed at 25 °C, and the flow rate was 50 μl/min. *Error bars* indicate S.D.
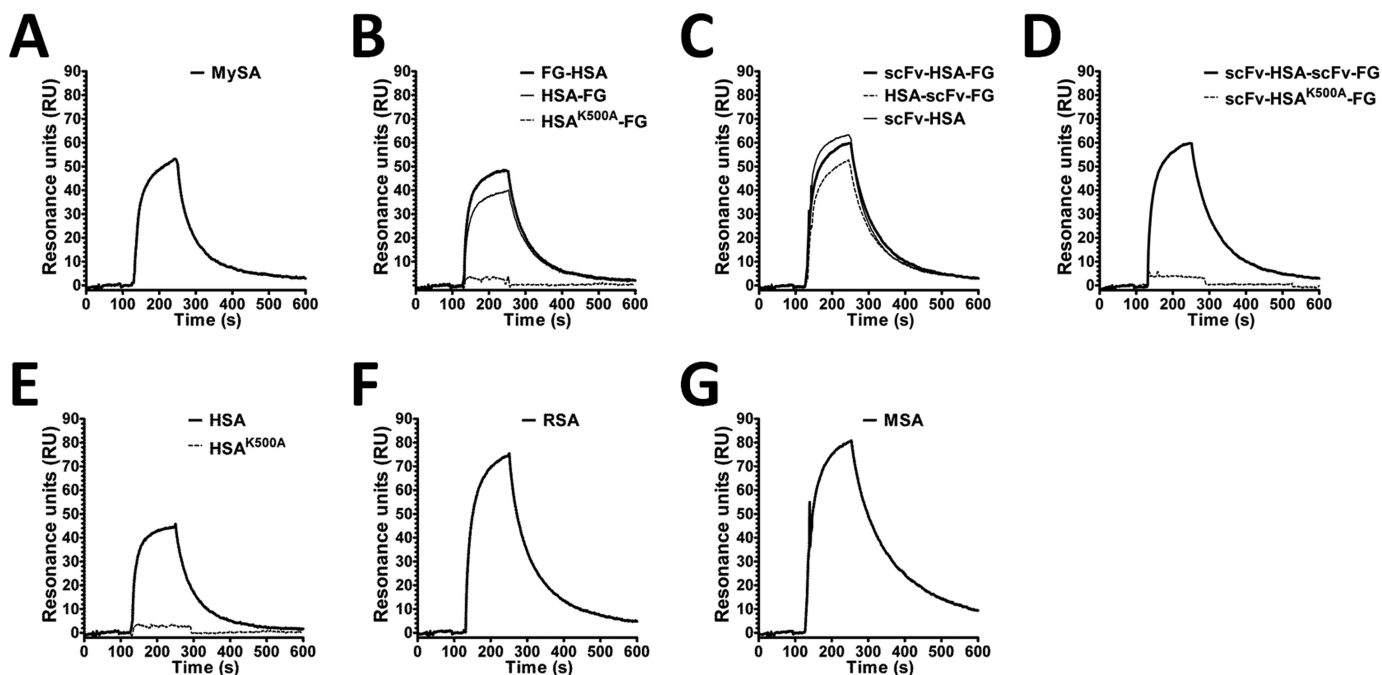

FIGURE 5. **Binding of albumin variants to rhesus monkey FcRn.** *A–G*, representative sensorgrams showing binding of 1 μM MySA (*A*), FG-HSA, HSA-FG, and HSA^{K500A}-FG (*B*), scFv-HSA-FG, HSA-scFv-FG, and scFv-HSA (*C*), scFv-HSA-scFv-FG and scFv-HSA^{K500A}-FG (*D*), HSA and HSA^{K500A} (*E*), RSA (*F*), and MSA (*G*) injected over myFcRn immobilized on a CM5 chip (~600 RU) at pH 6.0. Injections were performed at 25 °C, and the flow rate was 50 μl/min.

nal end of a protein of interest (Albufuse® technology). This strategy is independent of chemical cross-linking and has been broadly applied for half-life extension of small protein drugs with a molecular weight below the kidney clearance threshold, as reviewed (3, 20). However, the Albufuse® technology was developed before the recent understanding of the key role of FcRn in controlling the serum half-life of albumin (3, 14). Thus, the focus of this study was to investigate how genetic fusion to HSA affects binding to FcRn across species. In fact, this was important to address as we have recently shown that the C-terminal end of HSA is absolutely crucial for optimal binding to FcRn (15). Despite this, we show that fusion to either end of HSA has only minor impact on binding to the receptor. Specifically, fusion of a peptide or an scFv fragment to the N-terminal

end of HSA gave no reduction or only a minor reduction in binding affinity, whereas fusion to the C-terminal had a more pronounced effect.

Although the reduction in binding affinity was minor, and at most 2-fold, it may play a role *in vivo* when fusions are injected into animals or humans as it will compete for binding to FcRn in the presence of large amounts of endogenous albumin, amounting to roughly 40 mg/ml in both mouse and human. The ability of the fusions to compete for binding to the receptor is reflected by the competitive SPR binding data, where a slightly reduced capacity to compete for binding to hFcRn was observed as compared with WT HSA.

The importance of cross-species IgG binding differences to FcRn as a determining factor in circulatory half-life has been
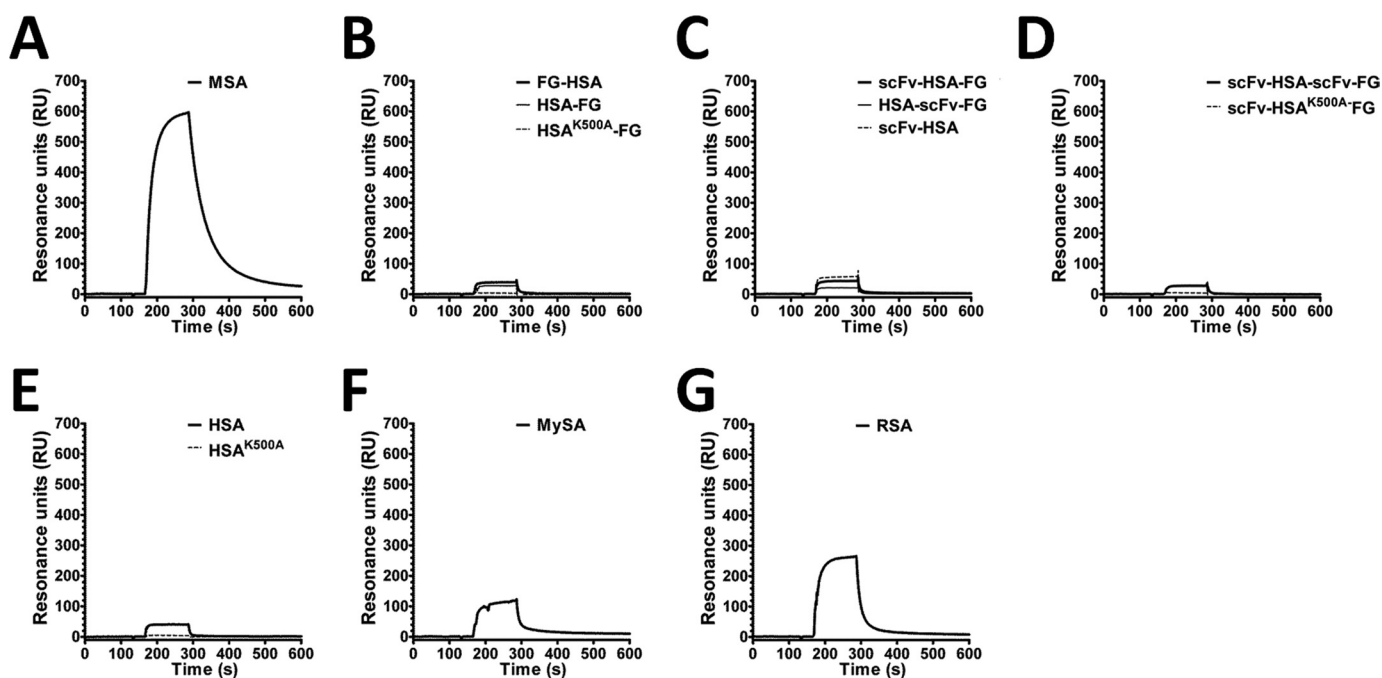
FIGURE 6. **Binding of albumin variants to mouse FcRn.** *A–G*, representative sensorgrams showing binding of 1 μM MSA (*A*), FG-HSA, HSA-FG, and HSA^{K500A}-FG (*B*), scFv-HSA-FG, HSA-scFv-FG, and scFv-HSA (*C*), scFv-HSA-scFv-FG and scFv-HSA^{K500A}-FG (*D*), HSA and HSA^{K500A} (*E*), MySA (*F*), and RSA (*G*) injected over mFcRn immobilized on a CM5 chip ($\sim$1000 RU) at pH 6.0. Injections were performed at 25 °C, and the flow rate was 50 μl/min.
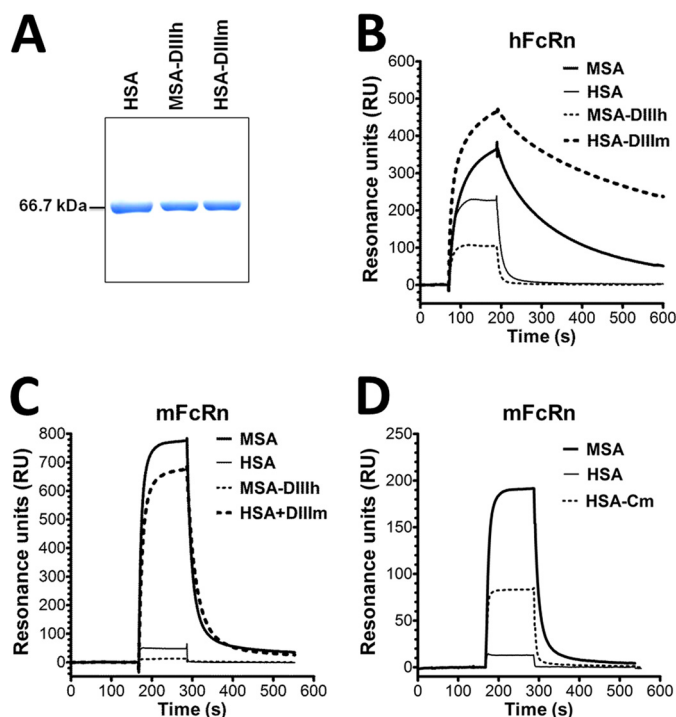

FIGURE 7. **Chimeric DIII albumin variants and their FcRn binding properties.** *A*, HSA, MSA-DIIIh, and HSA-DIIIm produced in *S. cerevisiae* and subsequently purified on an albumin affinity matrix were analyzed by 12% SDS-PAGE. *Lane 1* shows HSA, *lane 2* shows MSA-DIIIh, and *lane 3* shows HSA-DIIIm. *B* and *C*, representative sensorgrams showing binding of 1 μM HSA, MSA, MSA-DIIIh, and HSA-DIIIm injected over immobilized hFcRn ($\sim$800 RU) (*B*) and mFcRn ($\sim$1000 RU) (*C*), respectively, at pH 6.0, respectively. *D*, representative sensorgrams showing binding of 0.5 μM HSA, MSA, and HSA-Cm injected over immobilized mFcRn ($\sim$800 RU) at pH 6.0. Injections were performed at 25 °C, and the flow rate was 50 μl/min.

ever, they were rapidly cleared from the human circulation (29, 30). Recent knowledge has revealed that murine IgGs bind poorly to hFcRn, and thus, they are not rescued from degradation, a fact that explains their disappointingly short half-life in humans (22, 27, 28).

The half-life of biopharmaceuticals fused to HSA has been tested in rodents, and in all cases, fusion has resulted in improved pharmacokinetics, although the serum half-lives did not reach that of endogenous albumin of the animal used. This is also the case for scFv-HSA fusions evaluated in WT rats (25). We recently showed that MSA binds strongly to hFcRn, in stark contrast to the reduced binding of murine IgGs (22). The finding is supported by the fact that hFcRn transgenic mice that lack expression of endogenous FcRn show increased levels of MSA, indicative of reduced degradation (14). However, although human IgG binds strongly to mFcRn, HSA and fusions to HSA do not. The mouse form of FcRn prefers MSA over HSA and HSA fusions. This will necessarily affect *in vivo* preclinical evaluation in mice as small amounts of injected HSA fusion molecules will compete with large amounts of endogenous MSA for binding to mFcRn. We also show this to be the case for binding of HSA fusions to rFcRn, a finding that is supported by the fact that HSA has a half-life of only 15 h in rats, as compared with the 49 h of RSA (9).

The half-life enhancement observed for HSA fusions in rodents over that of the nonfused protein would appear predominantly to be the result of the increase in molecular weight, which for the fusions exceeds the kidney clearance threshold, and not an effect of FcRn-mediated rescue from degradation. Thus, rodents are limited for preclinical evaluation of WT HSA-based therapeutics whenever FcRn-mediated rescue is an issue. Ideally, both the genes encoding FcRn and albumin

appreciated for some time (22, 27, 28). The first generation of murine monoclonal IgGs, developed using the hybridoma technology, showed favorable half-life and activity in mice; how-

should be substituted with their human counterparts in a preferred mouse model.

We have previously shown that binding of hFcRn to DIII of HSA is a result of a pH-sensitive ionic network at the interaction interface, where two histidines found in FcRn (His-161 and His-166) and three within DIII of HSA (His-464, His-510, and His-535) are crucial for binding (13, 15). In addition, Lys-500, also found within HSA DIII, is a key player as mutation to alanine reduced binding by more than 30-fold (15). These residues are fully conserved among mouse, rat, rhesus monkey, and human. Here, we show that the swapping of DIII of MSA onto DI-DII of HSA gives rise to a chimeric variant with considerably improved binding to mFcRn, whereas swapping of DIII of HSA onto DI-DII of MSA reduced binding. This means that amino acids within DIII are important for the cross-species binding differences. However, sequence variations found outside DIII may also play a role, either directly or indirectly, as the chimeric variants did not obtain the binding profiles of their WT counterparts. Furthermore, swapping of the amino acids corresponding to the C-terminal α-helix from MSA onto HSA (HSA-Cm) resulted in a 4-fold improved binding as compared with WT HSA. Here, 8 out of 25 amino acids of the α-helix vary between the two species.

There is a great interest in engineering of IgG variants with improved pharmacokinetics through increased binding to FcRn at pH 6.0 and no binding at physiological pH (16, 31). Likewise, HSA mutants with such binding properties are expected to be recycled and rescued more efficiently than WT HSA and thus gain improved serum half-life. We have recently reported a docking model between HSA and hFcRn (15). The model did not include the last three amino acids of the C-terminal α-helix as the electron density corresponding to this part is not defined in crystal structures of albumin. Nevertheless, further dissection of DIII and the C-terminal end may lead to a new generation of HSA variants with greatly improved binding to hFcRn and extended half-life.

REFERENCES

1. Binz, H. K., Amstutz, P., and Plückthun, A. (2005) Engineering novel binding proteins from nonimmunoglobulin domains. *Nat. Biotechnol.* **23,** 1257–1268
2. McGregor, D. P. (2008) Discovering and improving novel peptide therapeutics. *Curr. Opin. Pharmacol.* **8,** 616–619
3. Andersen, J. T., and Sandlie, I. (2009) The versatile MHC class I-related FcRn protects IgG and albumin from degradation: implications for development of new diagnostics and therapeutics. *Drug Metab. Pharmacokinet.* **24,** 318–332
4. Harris, J. M., and Chess, R. B. (2003) Effect of pegylation on pharmaceuticals. *Nat. Rev. Drug Discov.* **2,** 214–221
5. Andersen, J. T., Pehrson, R., Tolmachev, V., Daba, M. B., Abrahmsén, L., and Ekblad, C. (2011) Extending half-life by indirect targeting of the neonatal Fc receptor (FcRn) using a minimal albumin binding domain. *J. Biol. Chem.* **286,** 5234–5241
6. Holt, L. J., Basran, A., Jones, K., Chorlton, J., Jespers, L. S., Brewis, N. D., and Tomlinson, I. M. (2008) Anti-serum albumin domain antibodies for extending the half-lives of short lived drugs. *Protein Eng. Des. Sel.* **21,** 283–288
7. Nguyen, A., Reyes, A. E., 2nd, Zhang, M., McDonald, P., Wong, W. L., Damico, L. A., and Dennis, M. S. (2006) The pharmacokinetics of an albumin-binding Fab (AB.Fab) can be modulated as a function of affinity for albumin. *Protein Eng. Des. Sel.* **19,** 291–297
8. Dennis, M. S., Zhang, M., Meng, Y. G., Kadkhodayan, M., Kirchhofer, D., Combs, D., and Damico, L. A. (2002) Albumin binding as a general strategy for improving the pharmacokinetics of proteins. *J. Biol. Chem.* **277,** 35035–35043
9. Smith, B. J., Popplewell, A., Athwal, D., Chapman, A. P., Heywood, S., West, S. M., Carrington, B., Nesbitt, A., Lawson, A. D., Antoniw, P., Eddelston, A., and Suitters, A. (2001) Prolonged *in vivo* residence times of antibody fragments associated with albumin. *Bioconjug. Chem.* **12,** 750–756
10. Müller, D., Karle, A., Meissburger, B., Höfig, I., Stork, R., and Kontermann, R. E. (2007) Improved pharmacokinetics of recombinant bispecific antibody molecules by fusion to human serum albumin. *J. Biol. Chem.* **282,** 12650–12660
11. Knudsen, L. B. (2010) Liraglutide: the therapeutic promise from animal models. *Int. J. Clin. Pract. Suppl.* 4–11
12. Chaudhury, C., Brooks, C. L., Carter, D. C., Robinson, J. M., and Anderson, C. L. (2006) Albumin binding to FcRn: distinct from the FcRn-IgG interaction. *Biochemistry* **45,** 4983–4990
13. Andersen, J. T., Dee Qian, J., and Sandlie, I. (2006) The conserved histidine 166 residue of the human neonatal Fc receptor heavy chain is critical for the pH-dependent binding to albumin. *Eur. J. Immunol.* **36,** 3044–3051
14. Chaudhury, C., Mehnaz, S., Robinson, J. M., Hayton, W. L., Pearl, D. K., Roopenian, D. C., and Anderson, C. L. (2003) The major histocompatibility complex-related Fc receptor for IgG (FcRn) binds albumin and prolongs its lifespan. *J. Exp. Med.* **197,** 315–322
15. Andersen, J. T., Dalhus, B., Cameron, J., Daba, M. B., Plumridge, A., Evans, L., Brennan, S. O., Gunnarsen, K. S., Bjørås, M., Sleep, D., and Sandlie, I. (2012) Structure-based mutagenesis reveals the albumin-binding site of the neonatal Fc receptor. *Nat. Commun.* **3,** 610
16. Ward, E. S., and Ober, R. J. (2009) Chapter 4: Multitasking by exploitation of intracellular transport functions the many faces of FcRn. *Adv. Immunol.* **103,** 77–115
17. Halpern, W., Riccobene, T. A., Agostini, H., Baker, K., Stolow, D., Gu, M. L., Hirsch, J., Mahoney, A., Carrell, J., Boyd, E., and Grzegorzewski, K. J. (2002) Albugranin, a recombinant human granulocyte colony stimulating factor (G-CSF) genetically fused to recombinant human albumin induces prolonged myelopoietic effects in mice and monkeys. *Pharm. Res.* **19,** 1720–1729
18. Subramanian, G. M., Fiscella, M., Lamousé-Smith, A., Zeuzem, S., and McHutchison, J. G. (2007) Albinterferon α-2b: a genetic fusion protein for the treatment of chronic hepatitis C. *Nat. Biotechnol.* **25,** 1411–1419
19. Makrides, S. C., Nygren, P. A., Andrews, B., Ford, P. J., Evans, K. S., Hayman, E. G., Adari, H., Uhlén, M., and Toth, C. A. (1996) Extended *in vivo* half-life of human soluble complement receptor type 1 fused to a serum albumin-binding receptor. *J. Pharmacol. Exp. Ther.* **277,** 534–542
20. Sleep, D., Cameron, J., and Evans, L. R. (April 29, 2013) Albumin as a versatile platform for drug half-life extension. *Biochim. Biophys. Acta* 10.1016/j.bbagen.2013.04.023
21. Andersen, J. T., Justesen, S., Fleckenstein, B., Michaelsen, T. E., Berntzen, G., Kenanova, V. E., Daba, M. B., Lauvrak, V., Buus, S., and Sandlie, I. (2008) Ligand binding and antigenic properties of a human neonatal Fc receptor with mutation of two unpaired cysteine residues. *FEBS J.* **275,** 4097–4110
22. Andersen, J. T., Daba, M. B., Berntzen, G., Michaelsen, T. E., and Sandlie, I. (2010) Cross-species binding analyses of mouse and human neonatal Fc receptor show dramatic differences in immunoglobulin G and albumin binding. *J. Biol. Chem.* **285,** 4826–4836
23. Berntzen, G., Lunde, E., Flobakk, M., Andersen, J. T., Lauvrak, V., and Sandlie, I. (2005) Prolonged and increased expression of soluble Fc receptors, IgG and a TCR-Ig fusion protein by transiently transfected adherent 293E cells. *J. Immunol. Methods* **298,** 93–104
24. Woodcock, D. M., Crowther, P. J., Doherty, J., Jefferson, S., DeCruz, E., Noyer-Weidner, M., Smith, S. S., Michael, M. Z., and Graham, M. W. (1989) Quantitative evaluation of *Escherichia coli* host strains for tolerance to cytosine methylation in plasmid and phage recombinants. *Nucleic Acids Res.* **17,** 3469–3478
25. Evans, L., Hughes, M., Waters, J., Cameron, J., Dodsworth, N., Tooth, D., Greenfield, A., and Sleep, D. (2010) The production, characterisation and enhanced pharmacokinetics of scFv-albumin fusions expressed in *Saccharomyces cerevisiae*. *Protein Expr. Purif.* **73,** 113–124

26. Payne, T., Finnis, C., Evans, L. R., Mead, D. J., Avery, S. V., Archer, D. B., and Sleep, D. (2008) Modulation of chaperone gene expression in mutagenized *Saccharomyces cerevisiae* strains developed for recombinant human albumin production results in increased production of multiple heterologous proteins. *Appl. Environ. Microbiol.* **74,** 7759–7766

27. Ober, R. J., Radu, C. G., Ghetie, V., and Ward, E. S. (2001) Differences in promiscuity for antibody-FcRn interactions across species: implications for therapeutic antibodies. *Int. Immunol.* **13,** 1551–1559

28. Vaccaro, C., Bawdon, R., Wanjie, S., Ober, R. J., and Ward, E. S. (2006) Divergent activities of an engineered antibody in murine and human systems have implications for therapeutic antibodies. *Proc. Natl. Acad. Sci. U.S.A.* **103,** 18709–18714

29. Köhler, G., and Milstein, C. (1975) Continuous cultures of fused cells secreting antibody of predefined specificity. *Nature* **256,** 495–497

30. Reichert, J. M. (2001) Monoclonal antibodies in the clinic. *Nat. Biotechnol.* **19,** 819–822

31. Roopenian, D. C., and Akilesh, S. (2007) FcRn: the neonatal Fc receptor comes of age. *Nat. Rev. Immunol.* **7,** 715–725